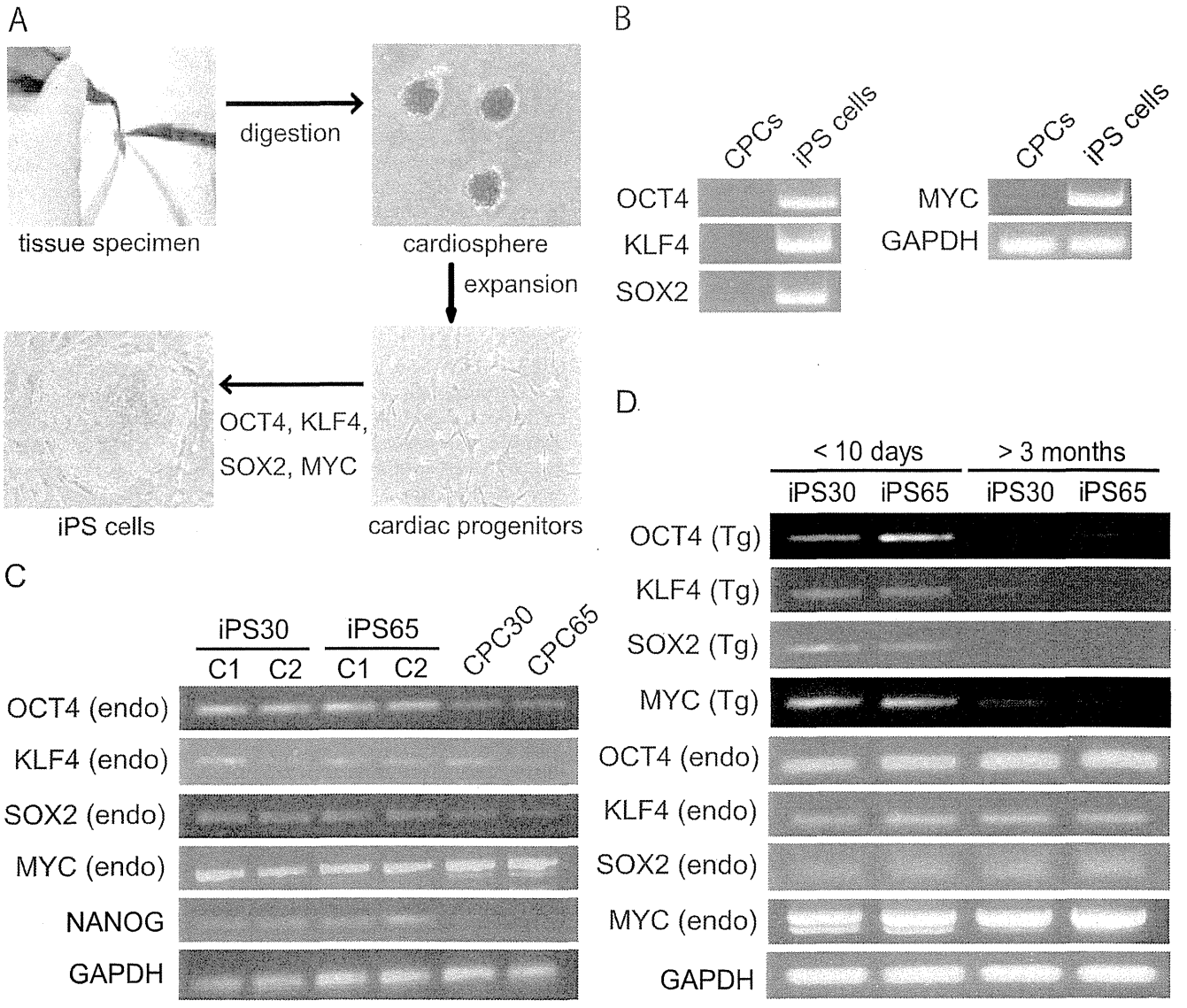

Figure 1. Reprogramming of disease-specific CPCs. (A) Schematic presentation of CPC isolation and iPS generation. (B) Retroviral transduction was verified by tagged-PCR and endogenous genes (C) are shown. (D) Retroviral silencing was confirmed during reprogramming after 3 months of infection. Trans- and endogenous-gene expressions are shown.
doi:10.1371/journal.pone.0102796.g001

CPCs, undifferentiated iPS cells, and differentiated iPS cells were cross-linked with 1% formaldehyde solution for 5 min at room temperature. The cells were harvested and nuclei were extracted, lysed, and enzymatically sheared to obtain chromatin. Immunoprecipitation was performed on an end-to-end rotation overnight at 4°C using the following antibodies: IgG (Upstate, Millipore 12-370), H3K4me2 (Upstate, Millipore 07-030), H3K27me3 (Upstate, Millipore 07-449), and acH3 (Upstate, Millipore 06-599). Crosslinking between DNA and proteins was reversed. DNA was purified after proteinase K digestion using Chromatin IP DNA Purification Kit (Active Motif). All precipitated DNA samples were amplified and quantitated by real-time PCR with SYBR Premix Ex Taq II (TaKaRa) and NKX2-5 ChIP primers (Table S2 in File S1). Signals corresponding to each antibody were normalized by respective input.

Promoter Assays

The TNNT2 (HPRM12846-PG04) and NPPA (natriuretic peptide A; HPRM23486-PG04) promoter activities were measured using a Dual Luminescence Assay Kit with a dual reporter construct containing Gaussia luciferase (GLuc) and secreted alkaline phosphatase (SEAP) side by side from a single sample (all from GeneCopoeia, Inc.). Each promoter is placed upstream of the GLuc reporter gene and contains a specific cardiac transcription factor as an insert. A secondary reporter gene SEAP was used to monitor the transfection efficiency for normalization. To detect serum response element (SRE) promoter activities, both SRE fragment (pGL4.33 [luc2P/SRE/Hygro], Promega) and pGL4.74 (hRluc/TK, Promega) were co-transfected into human cells by using X-tremeGene HP reagent (Roche). The relative expression of SRE (luc2P) construct was normalized using a control vector (hRluc) introduced into the same cells. Human cells were transfected with human NKX2-5 cDNA (SC122678), human NKX2-5 shRNA (short hairpin RNA; TR311165B), human

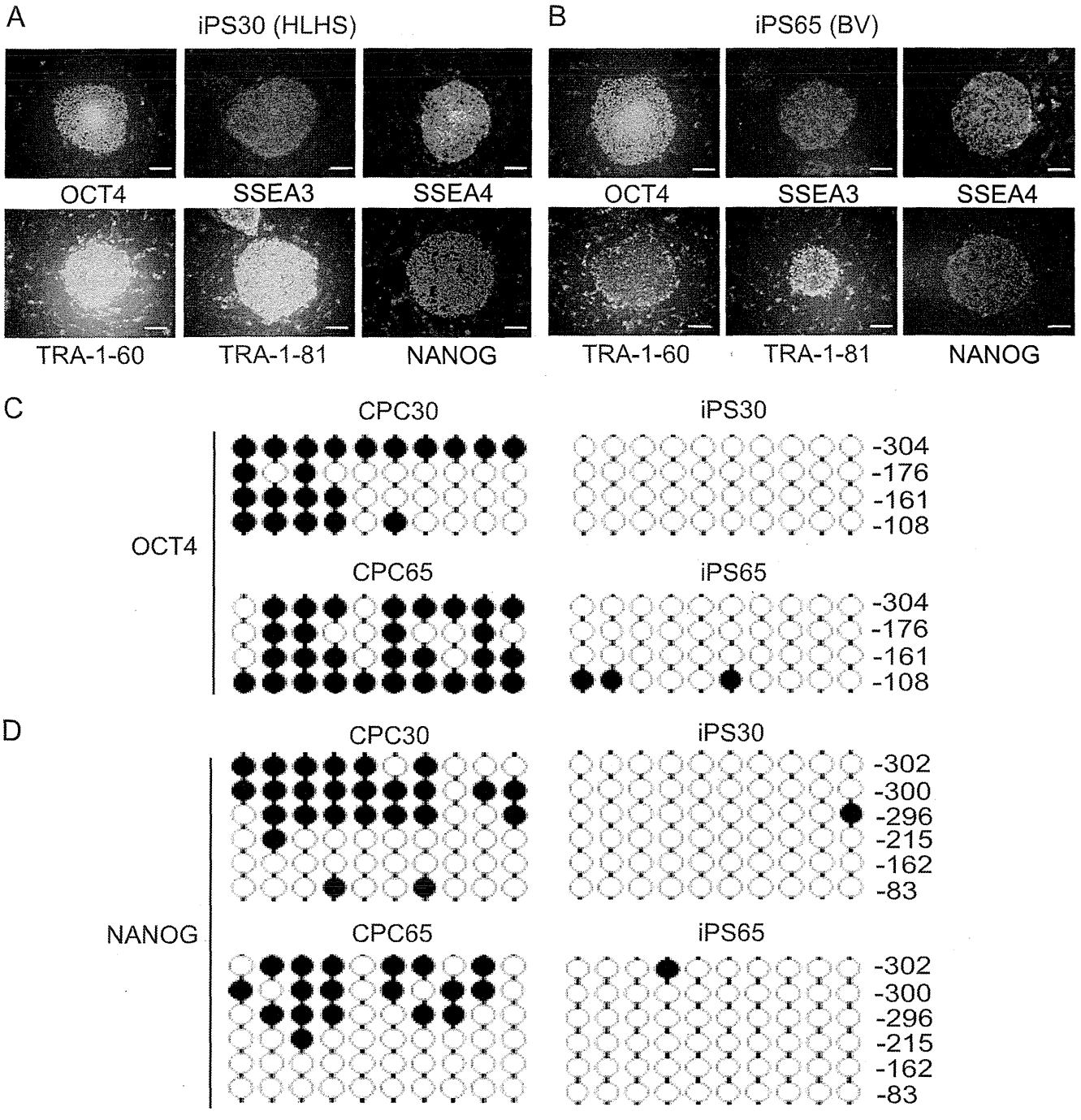

Figure 2. Characterization of disease-specific iPS cells. Representative patient-specific iPS clones at passage 10 (A, iPS30: HLHS; B, iPS65: TAPVC, representing BV). Colonies were stained with transcription factors typically expressed in iPS cells. Bar, 200 μm. (C and D) Bisulfite sequencing analysis of *OCT4* and *NANOG* promoter regions during reprogramming is shown. Closed and open circles represent methylated and unmethylated CpG dinucleotides, respectively.
doi:10.1371/journal.pone.0102796.g002

HAND1 cDNA (SC122690), human HAND1 shRNA (TR316857C), human NOTCH1 cDNA (SC308883), or human NOTCH1 shRNA (TR302916D) along with single- or dual-reporter constructs (all from OriGene Technologies, Inc.). The luciferase activities were measured by the Glomax-Multi+Detection System (Promega) 48 hours after transfection.

Statistics

Results are presented as the mean ± S.D. The significance of differences was evaluated by paired or unpaired Student's *t* test. A p value of less than 0.05 was considered significant.

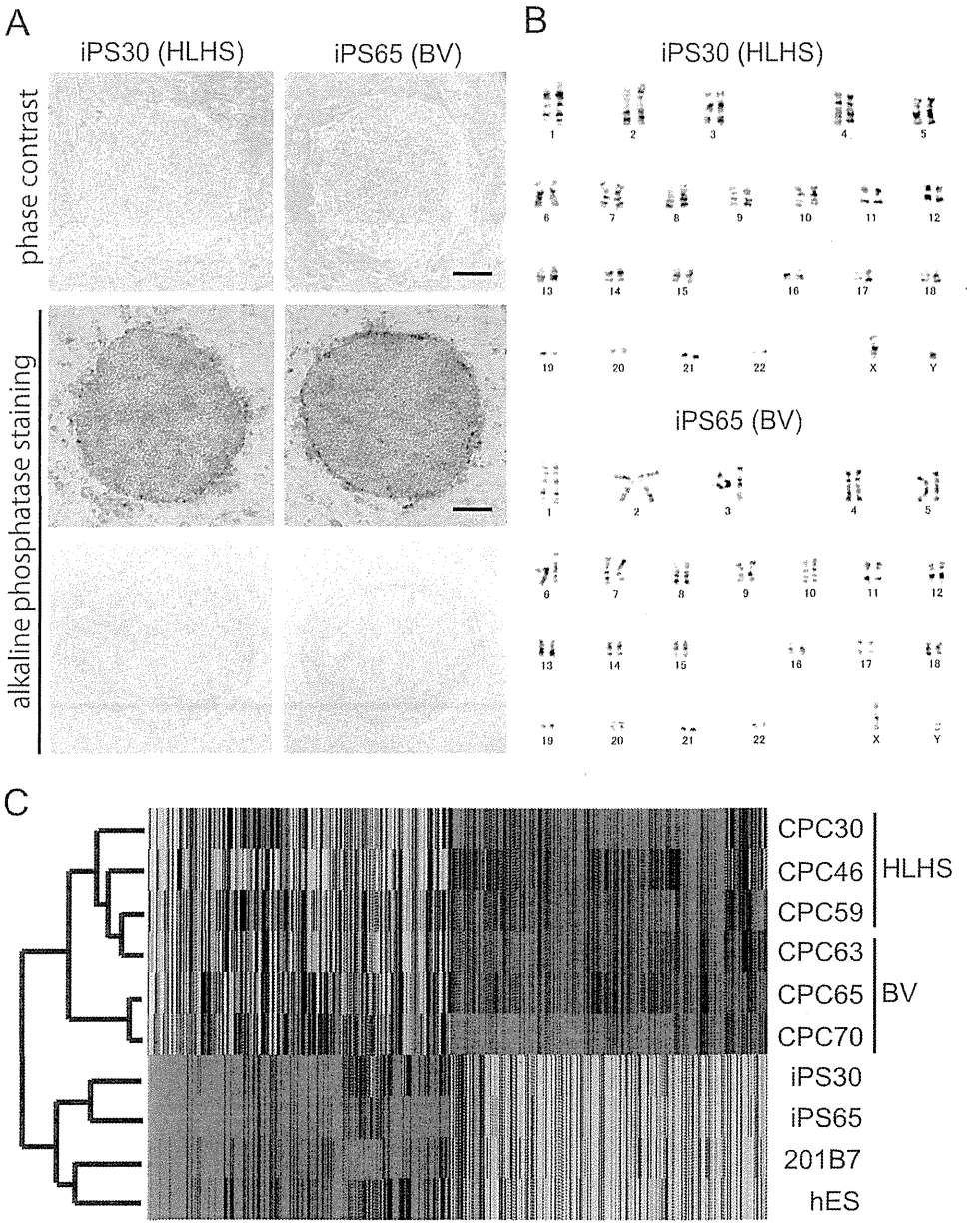

Figure 3. Patient-specific CPCs were fully reprogrammed. (A) Representative images of alkaline phosphatase staining are shown for iPS cells generated from HLHS (iPS30) and TAPVC representing BV (iPS65) patients. Bar, 200 μm. (B) Chromosomal abnormalities were not found in both iPS clones at 10 weeks by the G-banding method. (C) Heat map (right) and hierarchical cluster analysis (left) of global gene expression from patient-specific CPCs and iPS clones are shown. A commercially available 201B7 clone (Riken) was used as control human iPS cells.
doi:10.1371/journal.pone.0102796.g003

Results

Generation of Disease-Specific iPS Cells Using Patient-Derived CPCs

CPCs were isolated from the right atria of patients with congenital heart diseases undergoing cardiac surgery (Figure 1A). Individual cardiosphere-derived CPCs were isolated and infected with a combination of retroviruses encoding the transcription factors OCT4, KLF4, SOX2, and MYC as previously reported (Figure 1B) [11]. Among the iPS clones generated, five HLHS-iPS clones (iPS30, iPS46, iPS59, iPS68, and iPS72) and one BV-iPS clone (iPS65), obtained from a total anomalous pulmonary venous connection (TAPVC) patient, could propagate robustly when maintained on SNL feeder cells. We then used the iPS clones (iPS30-, iPS46-, and iPS72-HLHS) and the iPS65 clone (iPS-BV) for further evaluation in this study. Genomic integration of viral transgene was confirmed by RT-PCR. The reactivation of endogenous genes *OCT4* and *NANOG* led to higher levels in patient-specific iPS cells than in parental CPCs (Figure 1C). We also examined the expression of viral transgenes; RT-PCR showed that four factors (transgenes) were efficiently silenced in the established iPS cell lines; they were maintained for more than 15 passages and examined at 3 months post-infection (Figure 1D).

Characterization of Patient-Derived iPS Cells

The two types of disease-specific iPS cell grew at similar rates and uniformly expressed stringent pluripotent markers such as

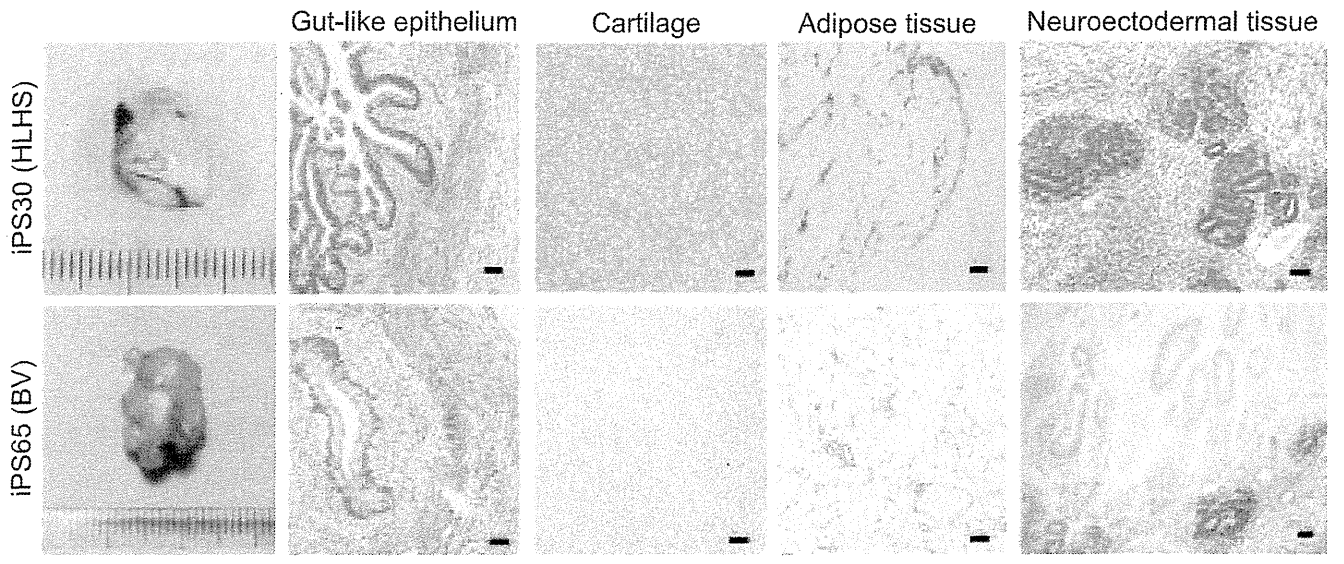

Figure 4. Patient-derived iPS cells differentiated into all three germ layer origins *in vivo*. Gross morphology and hematoxylin and eosin staining of patient-specific iPS cell-derived teratomas are shown. Teratomas were found in the testes of NOD/SCID mice 10 to 12 weeks after transplantation. Histological sections of identified cells represent all three germ layers. Bar, 50 μm.
doi:10.1371/journal.pone.0102796.g004

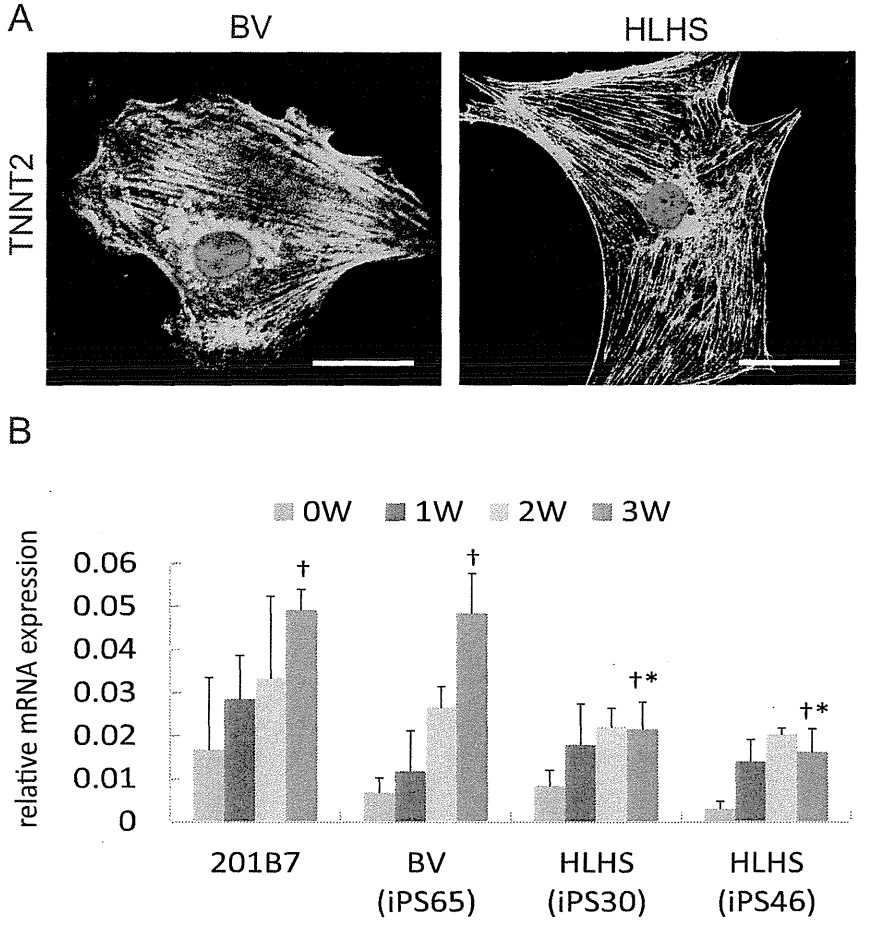

Figure 5. HLHS-derived iPS cells could give rise to cardiomyocytes. (A) Both HLHS- and BV-derived iPS cells could generate cardiac troponin-T (TNNT2)-positive cardiomyocytes (green) 3 weeks after lineage induction. Nuclei were shown by DAPI (blue). Bar, 30 μm. (B) Time course of TNNT2 expression in disease-specific iPS cells. Data were normalized using β2-microglobulin and human heart tissue for comparisons. *, $p<0.05$ vs. control and differentiated BV-derived iPS cells at 3 weeks. †, $p<0.05$ vs. before cardiac lineage induction (0 weeks) in each group.
doi:10.1371/journal.pone.0102796.g005

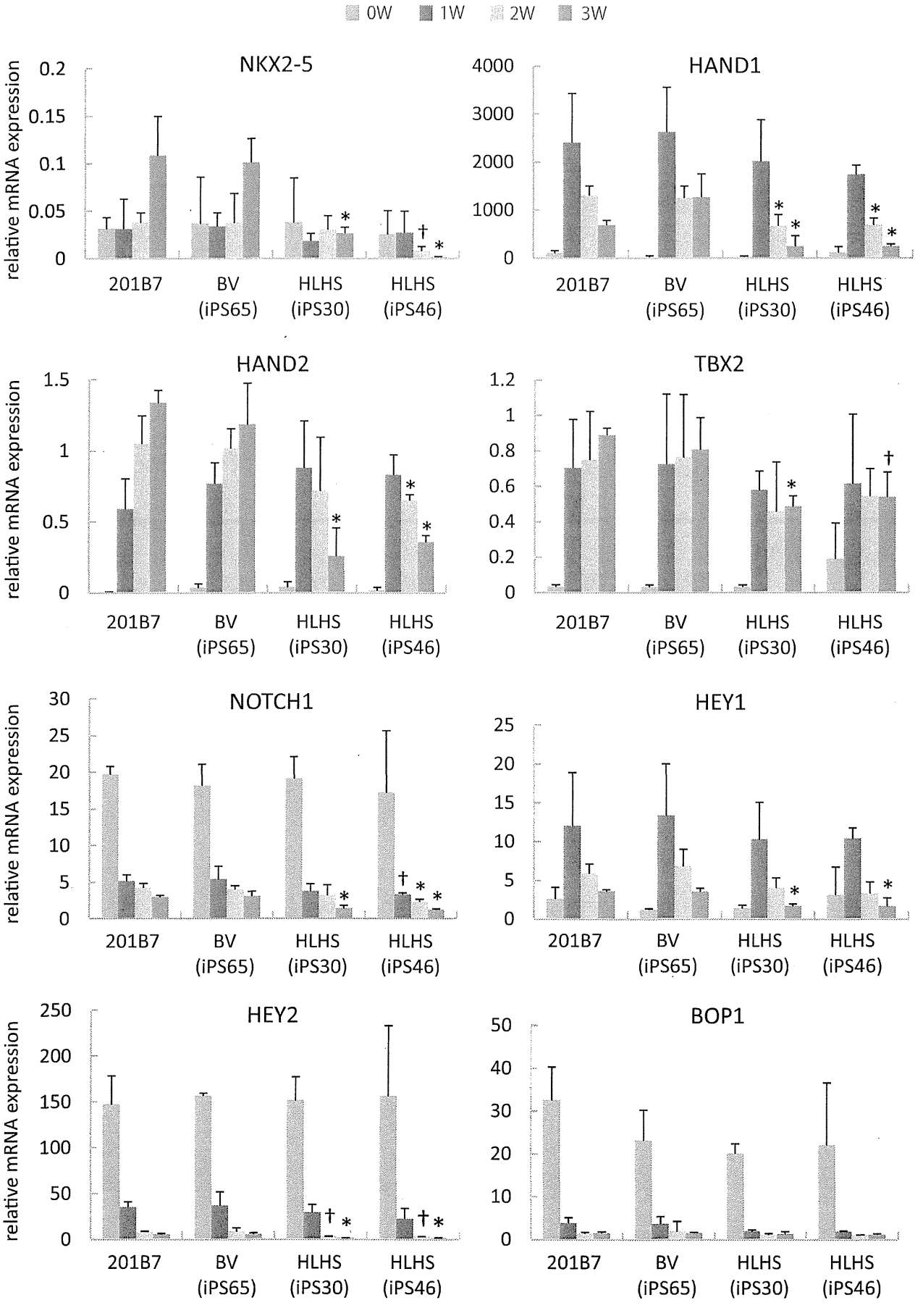
0W
1W
2W
3W
NKX2-5
HAND1
HAND2
TBX2
NOTCH1
HEY1
HEY2
BOP1
relative mRNA expression
201B7
BV (iPS65)
HLHS (iPS30)
HLHS (iPS46)

Figure 6. HLHS-iPS cell-derived cardiomyocytes showed decreased cardiac transcripts. mRNA expressions in control 201B7 iPS cells and one BV- and two HLHS-derived iPS cell lines during cardiac lineage induction at respective time points were determined by quantitative RT-PCR. All data were obtained from more than five independent experiments with three different clonal derivatives and normalized using β2-microglobulin and human heart tissue for comparisons. *, $p<0.05$ vs. differentiated 201B7 and BV-derived iPS cells at corresponding time points. †, $p<0.05$ vs. 201B7 at corresponding time points.
doi:10.1371/journal.pone.0102796.g006

OCT4, SSEA-3, SSEA-4, TRA-1-60, TRA-1-81, and NANOG, as determined by immunofluorescence (Figures 2A and B). We next sought to confirm the epigenetic reprogramming in individual iPS cells. Bisulfite sequencing analysis was performed to verify the degree of DNA methylation of the *OCT4* and *NANOG* promoters (Figures 2C and D). CpG dinucleotides in both promoter regions were highly demethylated in both patient-derived iPS cells relative to parental CPCs. Consistent with their ES-like morphology, both HLHS- and BV-derived iPS cells were positive for alkaline phosphatase staining (Figure 3A) and could maintain a normal karyotype for at least 10 weeks (Figure 3B).

Molecular Signatures of Patient-Derived CPCs and iPS Cells

We next performed global gene expression analysis on patient-specific iPS cells and parental CPCs using oligonucleotide microarray (Figure 3C). The heat map image showed that the expression profiles of both iPS cells were similar to those in control human iPS cells (clone 201B7) and human embryonic stem cells (clone khESC-1), but different from that in parental CPCs. Consistent with this, hierarchical clustering analysis demonstrated that disease-specific iPS cells closely resembled control human iPS cells, but were distinct from parental CPCs. Of particular note, pluripotency-associated genes represented by NANOG, POU5F1 (OCT4), and TDGF1 were expressed at remarkable levels in iPS cells compared with the levels in parental CPCs analyzed using three-independent CPC lines (Table S1 in File S1). Patient-derived CPCs significantly expressed typical gene transcripts indispensable for progenitor cell proliferation and differentiation, including IL1B, GREM1, LIF, TGFBR2, and IFGBP7 [12–15], and also showed a vascular-lineage-committed phenotype by expressing EDN1, LMO2, and VEGFC (Table S1 in File S1).

To assess the *in vivo* pluripotency, iPS cells generated from patients were injected into NOD/SCID mice. Ten to twelve weeks after transplantation, both iPS cells gave rise to teratomas originating from all three embryonic layers, including gut-like epithelia (endoderm), cartilage and adipose tissue (mesoderm), and neuroectodermal tissue (ectoderm) (Figure 4).

Cardiomyocyte Differentiation Potential of Disease-Specific iPS Cells

Upon cardiac differentiation, both HLHS- and BV-derived iPS cells generated cells that expressed typical cardiac structural proteins, cardiac troponin-T (TNNT2) verified by immunostaining, suggesting that HLHS-derived iPS cells are capable of generating cardiomyocytes *in vitro* (Figure 5A). Quantitative RT-PCR revealed that TNNT2 expression was significantly upregulated at 3 weeks after differentiation compared with that at baseline in both types of iPS-derived cardiomyocyte; however, HLHS-derived iPS cells showed reduced cardiomyogenic potential than those from control and BV heart (Fig. 5B).

Reduced Transcriptional Regulatory Programs During Cardiac Differentiation in HLHS-Derived iPS Cells

To determine whether HLHS-derived iPS cells have a distinct cardiac differentiation program, quantitative RT-PCR was performed. We found that cardiac transcriptional factors such as NKX2-5 and HAND1, known to drive cardiac growth and morphogenesis through primary heart field development, were significantly downregulated in HLHS-derived iPS cells at 2 to 3 weeks after differentiation compared with their levels in control 201B7 iPS- and BV-iPS-derived cardiomyocytes (Fig. 6) [16]. *HAND2* gene expression, which is known to preferentially control right heart morphogenesis but has a partially cumulative role with HAND1 in ventricular chamber formation, was also suppressed [17]. T-box transcription factor TBX2, a particularly important regulator for outflow tract cushion development and atrioventricular canal formation as myocardial patterning, was significantly reduced in differentiated HLHS-derived iPS cells [18]. In addition, reduced expression of NOTCH/HEY signaling was found. The decreased transcripts of these genes may be associated with obstruction in the inflow and outflow tracts seen in patients with HLHS due to the developmental defects in the regions of atrioventricular and outflow tract myocardium [19]. These data suggest that HLHS-derived iPS cells have the ability to give rise to cardiomyocytes; however, these cells had suppressed levels of indispensable genes involved in progenitor cell expansion and differentiation to initiate cardiogenesis, atrioventricular canal formation, and left ventricular outflow tract development to achieve functional ventricular growth.

NKX2-5, *HAND1*, and *NOTCH1* Are Indispensable to Restore the Activation of Cardiac-Specific Promoters in HLHS-Derived Cells

Next, we sought to determine whether *NKX2-5*, *HAND1*, and *NOTCH1* genes might be involved in the control of cardiac-specific promoter activities during the development of HLHS. Three possible targets of cardiac-related promoters, namely, SRE, TNNT2, and NPPA, were examined. To demonstrate that the generated shRNAs were specific for *NKX2-5*, *HAND1*, and *NOTCH1*, we performed transient transfection experiments to verify the inhibitory effects of respective gene expressions (Figure S1 in File S1). Four sets of shRNA for each gene were generated and transfected into HLHS-derived CPCs with either the full-length cDNA of interest or combined corresponding shRNA and cultured for 48 hours. Real-time RT-PCR analyses were performed to determine the appropriate ones for subsequent experiments. The inhibitory effects of selected shRNAs were confirmed by using additional clones of HLHS- and BV-derived CPCs (Figure S1 in File S1).

To investigate whether *NKX2-5*, *HAND1*, and *NOTCH1* might be the crucial transcriptional activators during cardiomyocyte differentiation, we performed co-transfection studies using the luciferase reporters driven by *SRE*, *TNNT2*, and *NPPA* promoters, respectively. As shown in Figures 7A and B, both HLHS-derived CPCs and iPS cells demonstrated a significant decrease in SRE transcriptional activation that was synergistically increased when NKX2-5, HAND1, and NOTCH1 were co-transfected into the cells, which was equivalent to the level in BV-derived cells without exogenous gene induction. To address whether these transcriptional factors are capable of suppressing endogenous SRE activation, we transfected shRNAs into BV-derived CPCs and found that either single shRNA or combina-

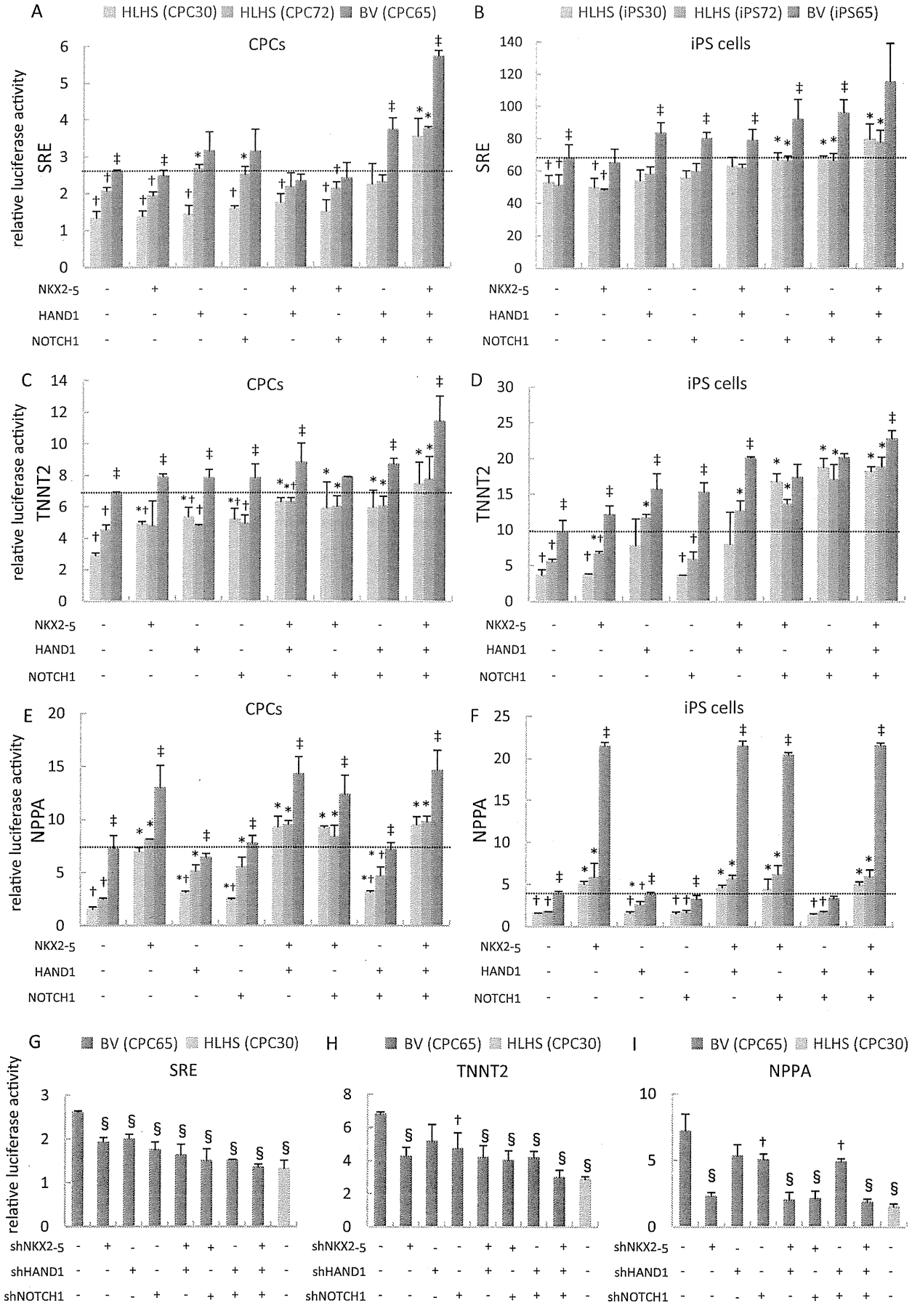
A
HLHS (CPC30)
HLHS (CPC72)
BV (CPC65)
CPCs
relative luciferase activity
SRE
NKX2-5
HAND1
NOTCH1
B
HLHS (iPS30)
HLHS (iPS72)
BV (iPS65)
iPS cells
C
TNNT2
D
E
NPPA
F
G
BV (CPC65)
HLHS (CPC30)
shNKX2-5
shHAND1
shNOTCH1
H
I

Figure 7. Synergistic restoration of target promoters by *NKX2-5, HAND1,* and *NOTCH* in HLHS-derived CPCs and iPS cells. Transcriptional activation of *SRE* promoter luciferase construct by combinatorial transfection of NKX2-5, HAND1, and NOTCH1 in HLHS- and BV-derived CPCs (A) or iPS cells (B). Co-transfection of *TNNT2* luciferase reporter with NKX2-5, HAND1, and NOTCH1 in CPCs (C) or iPS cells (D) is shown. *NPPA* luciferase construct was co-transfected with NKX2-5, HAND1, and NOTCH1 alone or in combination into CPCs (E) or iPS cells (F). (G-I) BV-derived CPCs were transfected with either control or shRNAs specific to inhibit NKX2-5, HAND1, and NOTCH1 expression. Results were normalized using an internal control (SEAP or hRluc) and obtained from more than triplicate sets of experiments. *, $p<0.05$ vs. the same HLHS sample without transfection of the gene of interest. †, $p<0.05$ vs. BV sample transfected with control vector alone. ‡, $p<0.05$ vs. both HLHS samples with the same treatment. §, $p<0.01$ vs. BV sample transfected with control vector alone.
doi:10.1371/journal.pone.0102796.g007

torial treatment had the potential to suppress SRE promoter activities (Figure 7G). We therefore hypothesized that these transcriptional factors may also participate in cardiomyocyte maturation. A *TNNT2* promoter-driven luciferase reporter was used in patient-derived CPCs and iPS cells with or without exogenous gene transfection. We found that BV-derived CPCs and iPS cells showed prominent *TNNT2* promoter activity compared with those in two independent HLHS-derived cells (Figures 7C and D). Induction of NKX2-5, HAND1, and NOTCH1 synergistically restored the reduced *TNNT2* transcriptional activation in both HLHS-derived CPCs and iPS cells. Loss-of-function studies using shRNAs showed that combinatorial inhibition of three genes, except for shHAND1 alone, could markedly suppress the *TNNT2* promoter activities (Figure 7H). *NPPA* promoter-driven luciferase assays demonstrated a striking finding that either *NKX2-5* alone or combinatorial gene transfection containing *NKX2-5* could fully restore the *NPPA* transcriptional activation in both HLHS-derived cell types (Figures 7E and F). This great impact of NKX2-5 on the *NPPA* promoter was confirmed by shRNA experiments that demonstrated that inhibition of NKX2-5 alone resulted in significant reduction of *NPPA* transcriptional activation in BV-derived CPCs (Figure 7I).

Histone Modification on *NKX2-5* Promoter in HLHS-Derived iPS cells

To investigate further whether epigenetic modifications, such as histone H3 methylation and acetylation, could be involved in transcriptional regulation in HLHS-derived iPS cells during cardiac-lineage induction, ChIP assay was performed using CPCs, undifferentiated iPS cells, and differentiated iPS cells. Although there were no differences in methylation or acetylation modification at histone H3 in CPCs and undifferentiated iPS cells derived from HLHS and BV patients, a marked decrease in dimethylated histone H3-lysine 4 (H3K4me2) and acetylated histone H3 (acH3) was found within the *NKX2-5* promoter regions in differentiated HLHS-derived iPS cells compared with those from a BV patient. We also identified significantly increased trimethylated H3-lysine 27 (H3K27me3) in the differentiated HLHS-derived iPS cells (Figure 8).

Discussion

Congenital heart disease involves abnormalities in cardiac structure or function that arise before birth. Although a number of studies have uncovered that heterozygous mutations in cardiac regulatory genes caused congenital heart defects in humans, the identified genetic variants may not be directly correlated with biological insights that potentially contribute to disease development [20]. In lower vertebrates, the key regulatory mechanisms involved in early heart morphogenesis have been investigated extensively, but our understanding of the causal genes responsible for the development of such complex disease is still limited in humans [16]. Recent progress in stem cell biology has revealed a previously unappreciated aspect of cardiac morphogenesis that is genetically controlled by a series of lineage-restriction steps of common progenitor cells that arise from the primary cardiac crescent during development [21]. In this study, we employed an integrated approach by using patient-derived iPS cells to study the pathogenesis of HLHS in order to uncover the molecular fingerprints that may control progenitor cell fate during early cardiac development.

Endogenous CPCs from adult mammalian heart were identified a decade ago [22,23]. Although human CPCs can also be used in cell culture to dissect the molecular mechanisms underlying congenital heart defects, investigation of inductive signals associated with early cardiogenesis by using postnatal cells, obtained after the onset of the disease of interest, may not be appropriate for the definitive identification of genes responsible for early developmental defects. In addition, it may not be possible to recapitulate the phenotypes by CPCs as *in vitro* sources because the pathogenesis of these complex diseases may require multiple cell types to initiate disease development. Reprogramming technology may facilitate disease investigation by assessing a wide variety of pluripotent stem cell differentiation pathways, including cardiomyogenic commitment, rather than by tracking the lineage-restricted progenitor cell fate. In this regard, patient-specific iPS cells may represent a promising cell source to study disease mechanisms.

There are several limitations in this study. The generation of patient-derived iPS cells remains technically demanding and clonal variation within patients or clones from other patients could be seen among studies; as such, their pathogenetic heterogeneity should not be ruled out. The lack of patients and control samples needs to be further emphasized and acknowledged could be a major limitation in this study. Whether the *in vitro* observations at 3 weeks after iPS cell differentiation could be used as a compatible model of embryonic heart development in humans remain unclear, so the obtained results may need to be interpreted with caution. Ethical concerns have limited the use of human CPCs isolated from healthy individuals due to the safety issues that must be considered during cardiac biopsy procedures. Our approach of using myocardial tissue specimens obtained during cardiac surgery in children was absolutely safe without any appearance of defects compared with the common skin biopsy procedures. With respect to a control, 201B7 iPS cells were used for comparative analysis in this study. We have also isolated disease-derived CPCs from a TAPVC patient in whom the pulmonary veins fail to enter the left atrium but supply the blood flow into the right atrium. Besides the malpositioned pulmonary vessels in this case, four-chamber morphogenesis and outflow tract developed normally in the presence of patent foramen ovale to support oxygenation.

In this study, we found a series of transcriptional repression during the directed differentiation of HLHS-derived iPS cells, which are implicated in the development of HLHS (Figure 9A) and mutually controlled by a core-transcriptional regulatory network, including NKX2-5 and HAND [16]. These results are consistent with a previous mouse study demonstrating that the Nkx2-5-Hand1 transcriptional pathway plays an essential role in

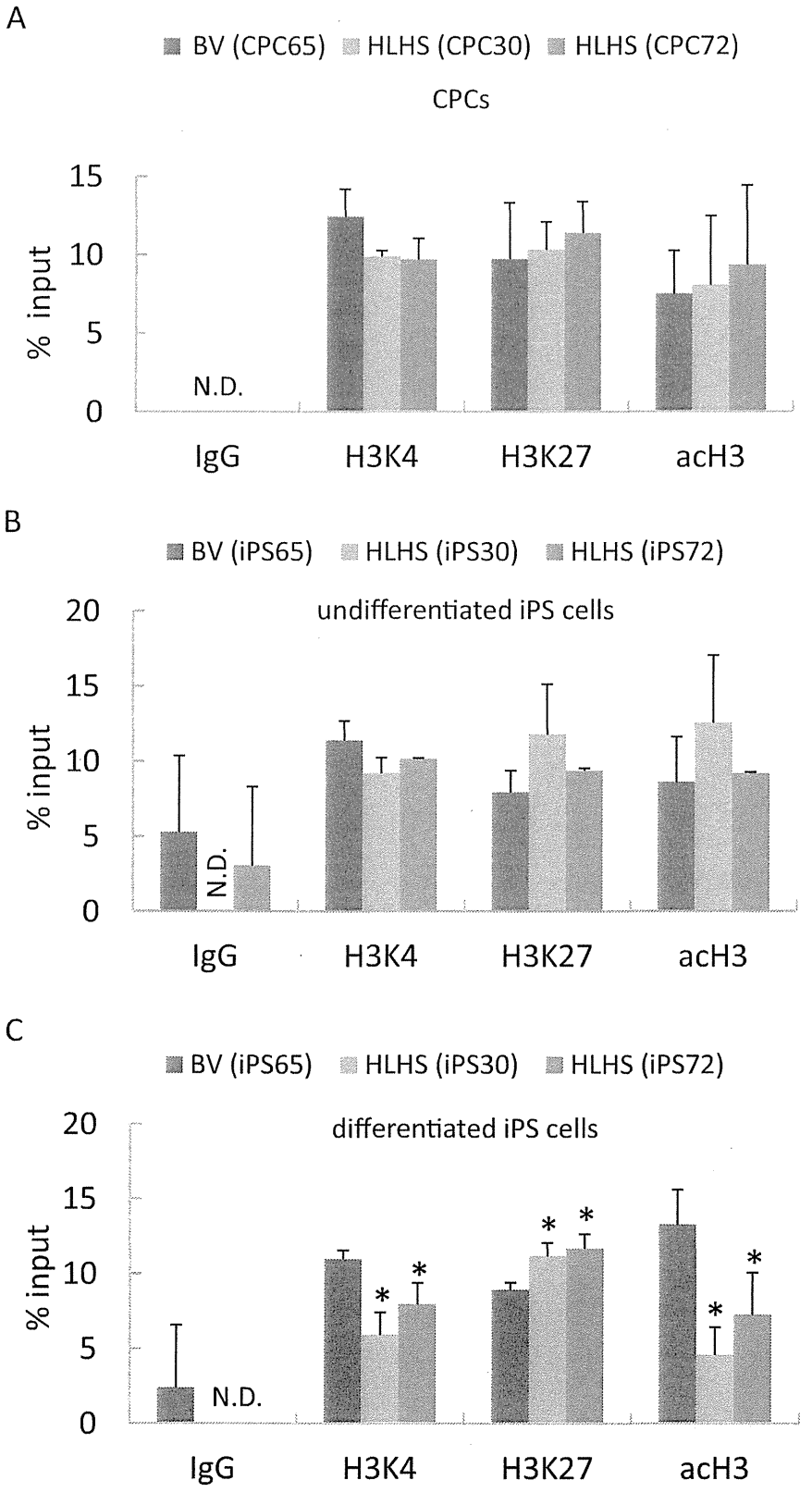

Figure 8. HLHS-iPS cell-derived cardiomyocytes showed suppressed H3K4 methylation and H3 acetylation, but increased H3K27 methylation. Undifferentiated CPCs (A) and iPS cells (B) and differentiated (cardiac-lineage induction for 3 weeks) iPS cells (C) were analyzed by ChIP assay. N.D., not detected; *, $p<0.05$ vs. differentiated BV-derived iPS cells. Data are expressed as the percentage of input DNA.
doi:10.1371/journal.pone.0102796.g008

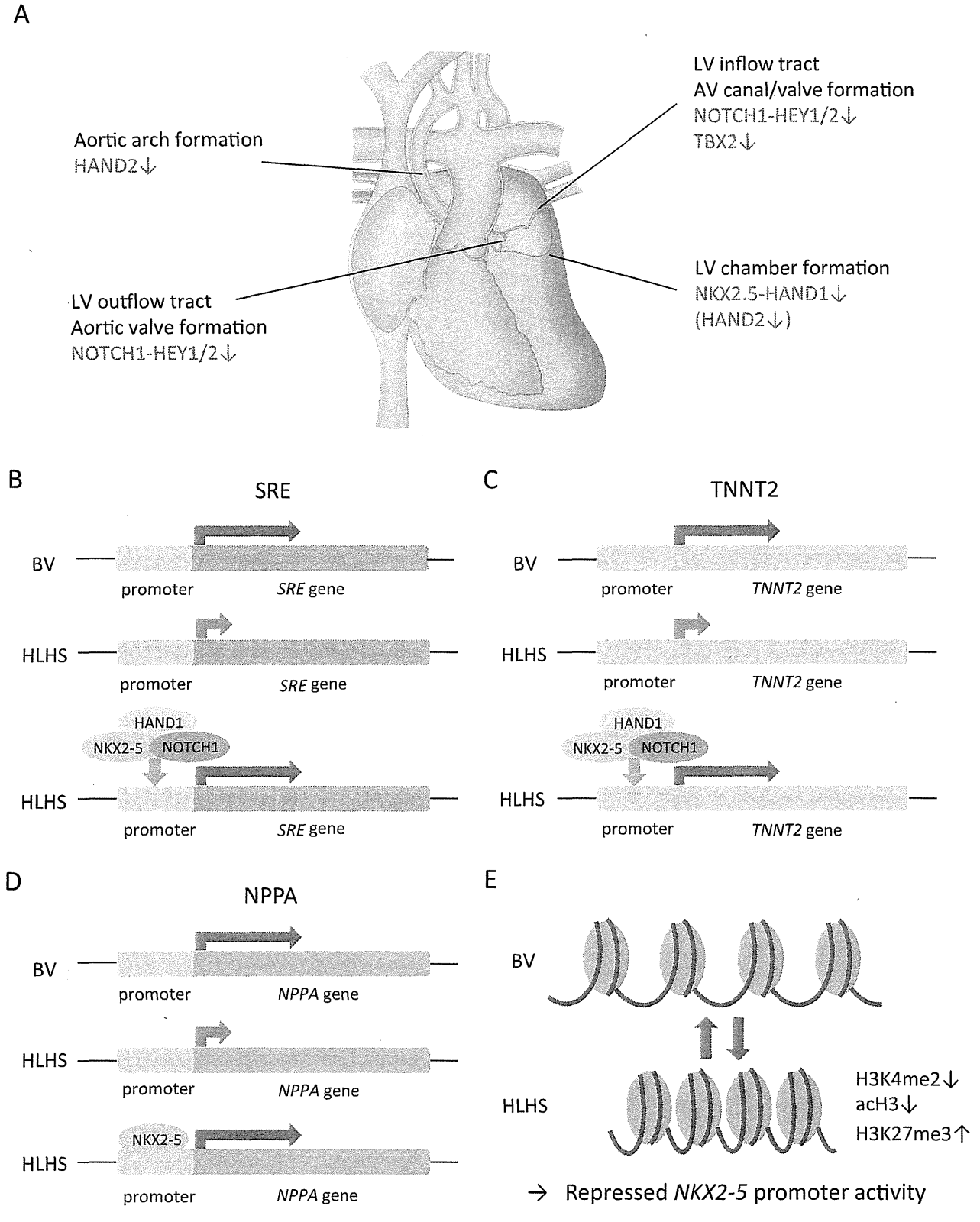

Figure 9. Orchestrated gene regulatory network in the development of HLHS. (A) Core transcriptional factors expressed in cardiac progenitor cells serve as targets in response to inductive signals to initiate cardiogenesis. NKX2-5 is predominantly expressed in the primary heart field and controls progenitor cell proliferation. Genes regulate atrioventricular (AV) canal and valve development. Reduced expression may contribute to mitral- and aortic-valve stenosis/atresia often seen in HLHS. NOCTH modulates left heart outflow tract development and the resultant obstruction may cause secondary ventricle hypoplasia. HAND1/2 specify left and right ventricular chamber morphogenesis, and the absence of these genes may lead to a hypoplastic ventricle. (B–D) Schematic diagrams of *SRE*, *TNNT2*, and *NPPA* transcriptional activation. HLHS-derived CPCs and iPS cells showed significantly reduced luciferase activities compared with BV-derived cells. Co-transfection analysis of reporter constructs with NKX2-5, HAND1, and

NOTCH1, proposed core transcriptional factors, could synergistically restore the transcriptional activation in these reporters equivalent to the levels in BV-derived cells. (E) Major chromatin features in differentiated HLHS- and BV-derived iPS cells are shown. Upon cardiomyocyte differentiation, HLHS-derived iPS cells failed to enrich the active histone marks such as H3K4me2 and acH3, whereas repressive histone marks such as H3K27me3 increased, resulting in compact chromatin that lost enhancer marks and gained repressor marks on the *NKX2-5* promoter.
doi:10.1371/journal.pone.0102796.g009

left ventricular formation during cardiogenesis [24]. Of particular note, potential *NKX2-5* mutations were found in patients with HLHS [25,26] and a frameshift mutation in *HAND1* was reported [27]. The epigenetic signature of *NKX2-5* transcripts in iPS cells during differentiation is unknown [28]. In general, undifferentiated stem cells show hypomethylation of specific gene promoters to allow their rapid activation during the processes of differentiation. Methylation at H3K4 is associated with transcriptional activation, whereas H3K27me3 represents a suppressive mark of condensed chromatin status. The results of ChIP assay suggest that reduced H3K4me2 and increased H3K27me3 on the *NKX2-5* promoter might be the alternative epigenetic mechanism to interpret the impaired transcriptional expression found in the differentiation processes of HLHS-derived iPS cells.

The atrioventricular canal is located between atrial and ventricular chamber regions and is an essential source to complete endocardial cushion and valve development. Decreased inflow dynamics may lead to mitral stenosis/atresia as seen in HLHS. Although we did not observe significant changes in BOP1, which is a signaling control of secondary heart field development, combinatorial contributions by the NOTCH/HEY and TBX2 axes from both heart fields might specify this process in HLHS (Figure 9A) [18,29,30].

HLHS generally involves a predisposition to obstructed left ventricular outflow, which is commonly associated with aortic atresia [31]. The pathogenesis of HLHS may originate as a primary defect in valve development that leads to secondary LV hypoplasia (Figure 9A). *NOTCH1* mutations have been identified in HLHS individuals and aortic valve anomalies [32,33]. Recent study related to *NOTCH1* mutations in humans suggests a direct function of activated NOTCH and NOTCH ligand JAGGED complex in controlling myocardial growth through *NKX2-5* activation [34,35]. The most prominent NOTCH effectors are basic helix-loop-helix transcription factors, HEY1/2. Endocardial NOTCH/HEY signal integration during endocardial to mesenchymal transition has been shown to be critical in the generation of cardiac valve as a specialized structure [36]. Finally, HAND1 and HAND2 are preferentially expressed in primary and secondary heart fields to develop left and right chamber morphogenesis [37,38]. Although the role of Hand2 is generally essential in the secondary heart field [39], it was reported that the decreased expression of Hand2 in mice could influence formation of the LV and the aortic arch system [24], suggesting some implications in the phenotype of HLHS.

In this study, HLHS-derived iPS cells demonstrated lower capability of differentiating into cardiomyocytes (Figure 5B), which is consistent with a recent report showing that iPS cells generated from HLHS patients had impaired sarcomeric organization as well as altered calcium transient patterning and responses to β-adrenergic antagonist during differentiation when compared with control iPS and human ES cells [40]. These observations indicate that HLHS-derived cells may have critical defects of transcriptional activation that are required for cardiac differentiation and organ morphogenesis of the heart. Among the genes analyzed in this study, *NKX2-5*, *HAND1*, and *NOTCH1* were identified to be the essential transcripts to activate a subset of cardiac lineage-specific gene transcription. In contrast, the transcripts of GATA4 and TBX5 have been shown to be cooperatively involved in directing early cardiac transcriptional activation in vitro and in vivo; indeed, we only observed comparable expression of these genes between HLHS- and BV-derived cells during cardiac differentiation (data not shown) [41,42]. Novel insights have come from the gain- and loss-of-function experiments that demonstrated that these three transcription factors synergistically regulated *SRE*, *TNNT2*, and *NPPA* transcriptional activation (Figure 9B–D). Although the chromatin states of tissue-specific stem cells have been shown to be intermediate between pluripotent and differentiated cells [43], we found that HLHS-iPS-derived cardiomyocytes but not undifferentiated CPCs failed to acquire active histone marks at the *NKX2-5* promoter region to achieve full cardiac-lineage induction compared with BV-derived iPS cells (Figure 9E). These results suggest that epigenetic pre-patterning during development may also contribute to reduced cardiac-lineage specification and impaired heart morphogenesis in HLHS.

In conclusion, patient-derived CPCs can be efficiently reprogrammed into disease-specific iPS cells for modeling congenital heart malformations. This integrated technology offers an unprecedented opportunity to reveal the genes differentially expressed between iPS cells with and without ventricular chamber defects and might enable correction of the gene variants for therapeutic purposes in HLHS. With knowledge of early cardiac development, the molecular regulatory networks that mediate myocardial growth and morphogenesis can be more informatively dissected by using patient-derived iPS cells.

Supporting Information

File S1 File contains Figure S1 and Tables S1 and S2. Figure S1. Verification of inhibitory effects of shRNAs for NKX2-5, HAND1, and NOTCH1 in CPCs. (A) HLHS-derived CPCs were cultured in growth medium and transfected with transcriptional factors as indicated with or without corresponding four sets of shRNAs. The inhibitory effects for each gene were confirmed by real-time RT-PCR. (B) The most efficient shRNA for each gene was selectively used to inhibit endogenous expression of transcription factors in BV-derived CPCs. Full length of cDNA for each transcription factor was transfected into HLHS-derived CPCs and the repressive effect was examined. Data were obtained from more than five-independent experiments and normalized by using β2-microglobulin and human heart tissue for comparisons. *, $p<0.05$ vs. sample transfected with gene of interest alone. †, $p<0.05$ vs. sample without shRNA transfection. **Table S1. Expression of embryonic development-associated genes in patient-derived CPCs and their iPS cell derivatives during reprogramming. Table S2. Primers used for RT-PCR, quantitative RTPCR, bisulfite sequencing analysis, and ChIP assay.**
(DOC)

Acknowledgments

The RNA used for global gene expression analysis was a kind gift from K. Fukuda (Keio University School of Medicine) and was isolated by F. Hattori (Keio University School of Medicine) from a human ES cell line (khESC-1), as previously reported [7].

Author Contributions

Conceived and designed the experiments: HO. Performed the experiments: JK MY ST. Analyzed the data: JK MY YN HO. Contributed reagents/materials/analysis tools: MH YN SK KN HI SS. Wrote the paper: HO.

References

1. Sano S, Ishino K, Kawada M, Arai S, Kasahara S, et al. (2003) Right ventricle-pulmonary artery shunt in first-stage palliation of hypoplastic left heart syndrome. J Thorac Cardiovasc Surg 126: 504–509.
2. Barron DJ, Kilby MD, Davies B, Wright JG, Jones TJ, et al. (2009) Hypoplastic left heart syndrome. Lancet 374: 551–564.
3. Lamour JM, Kanter KR, Naftel DC, Chrisant MR, Morrow WR, et al. (2009) The effect of age, diagnosis, and previous surgery in children and adults undergoing heart transplantation for congenital heart disease. J Am Coll Cardiol 54: 160–165.
4. Hinton RB, Martin LJ, Rame-Gowda S, Tabangin ME, Cripe LH, et al. (2009) Hypoplastic left heart syndrome links to chromosomes 10q and 6q and is genetically related to bicuspid aortic valve. J Am Coll Cardiol 53: 1065–1071.
5. Iascone M, Ciccone R, Galletti L, Marchetti D, Seddio F, et al. (2011) Identification of de novo mutations and rare variants in hypoplastic left heart syndrome. Clin Genet.
6. Narsinh K, Narsinh KH, Wu JC (2011) Derivation of human induced pluripotent stem cells for cardiovascular disease modeling. Circ Res 108: 1146–1156.
7. Hattori F, Chen H, Yamashita H, Tohyama S, Satoh YS, et al. (2010) Nongenetic method for purifying stem cell-derived cardiomyocytes. Nat Methods 7: 61–66.
8. Tateishi K, Ashihara E, Honsho S, Takehara N, Nomura T, et al. (2007) Human cardiac stem cells exhibit mesenchymal features and are maintained through Akt/GSK-3beta signaling. Biochem Biophys Res Commun 352: 635–641.
9. Takehara N, Tsutsumi Y, Tateishi K, Ogata T, Tanaka H, et al. (2008) Controlled delivery of basic fibroblast growth factor promotes human cardiosphere-derived cell engraftment to enhance cardiac repair for chronic myocardial infarction. J Am Coll Cardiol 52: 1858–1865.
10. Park IH, Lerou PH, Zhao R, Huo H, Daley GQ (2008) Generation of human-induced pluripotent stem cells. Nat Protoc 3: 1180–1186.
11. Takahashi K, Tanabe K, Ohnuki M, Narita M, Ichisaka T, et al. (2007) Induction of pluripotent stem cells from adult human fibroblasts by defined factors. Cell 131: 861–872.
12. Wang L, Liu Z, Balivada S, Shrestha T, Bossmann S, et al. (2012) Interleukin-1beta and transforming growth factor-beta cooperate to induce neurosphere formation and increase tumorigenicity of adherent LN-229 glioma cells. Stem Cell Res Ther 3: 5.
13. Sneddon JB, Zhen HH, Montgomery K, van de Rijn M, Tward AD, et al. (2006) Bone morphogenetic protein antagonist gremlin 1 is widely expressed by cancer-associated stromal cells and can promote tumor cell proliferation. Proc Natl Acad Sci U S A 103: 14842–14847.
14. Zhao X, Malhotra GK, Lele SM, Lele MS, West WW, et al. (2010) Telomerase-immortalized human mammary stem/progenitor cells with ability to self-renew and differentiate. Proc Natl Acad Sci U S A 107: 14146–14151.
15. Yamamoto A, Shofuda T, Islam MO, Nakamura Y, Yamasaki M, et al. (2009) ABCB1 is predominantly expressed in human fetal neural stem/progenitor cells at an early development stage. J Neurosci Res 87: 2615–2623.
16. Olson EN (2006) Gene regulatory networks in the evolution and development of the heart. Science 313: 1922–1927.
17. McFadden DG, Barbosa AC, Richardson JA, Schneider MD, Srivastava D, et al. (2005) The Hand1 and Hand2 transcription factors regulate expansion of the embryonic cardiac ventricles in a gene dosage-dependent manner. Development 132: 189–201.
18. Greulich F, Rudat C, Kispert A (2011) Mechanisms of T-box gene function in the developing heart. Cardiovasc Res 91: 212–222.
19. Rutenberg JB, Fischer A, Jia H, Gessler M, Zhong TP, et al. (2006) Developmental patterning of the cardiac atrioventricular canal by Notch and Hairy-related transcription factors. Development 133: 4381–4390.
20. Bruneau BG (2008) The developmental genetics of congenital heart disease. Nature 451: 943–948.
21. Epstein JA (2010) Franklin H. Epstein Lecture. Cardiac development and implications for heart disease. N Engl J Med 363: 1638–1647.
22. Beltrami AP, Barlucchi L, Torella D, Baker M, Limana F, et al. (2003) Adult cardiac stem cells are multipotent and support myocardial regeneration. Cell 114: 763–776.
23. Oh H, Bradfute SB, Gallardo TD, Nakamura T, Gaussin V, et al. (2003) Cardiac progenitor cells from adult myocardium: homing, differentiation, and fusion after infarction. Proc Natl Acad Sci U S A 100: 12313–12318.
24. Yamagishi H, Yamagishi C, Nakagawa O, Harvey RP, Olson EN, et al. (2001) The combinatorial activities of Nkx2.5 and dHAND are essential for cardiac ventricle formation. Dev Biol 239: 190–203.
25. Elliott DA, Kirk EP, Yeoh T, Chandar S, McKenzie F, et al. (2003) Cardiac homeobox gene NKX2-5 mutations and congenital heart disease: associations with atrial septal defect and hypoplastic left heart syndrome. J Am Coll Cardiol 41: 2072–2076.
26. McElhinney DB, Geiger E, Blinder J, Benson DW, Goldmuntz E (2003) NKX2.5 mutations in patients with congenital heart disease. J Am Coll Cardiol 42: 1650–1655.
27. Reamon-Buettner SM, Ciribilli Y, Inga A, Borlak J (2008) A loss-of-function mutation in the binding domain of HAND1 predicts hypoplasia of the human hearts. Hum Mol Genet 17: 1397–1405.
28. Pasini A, Bonafe F, Govoni M, Guarnieri C, Morselli PG, et al. (2013) Epigenetic signature of early cardiac regulatory genes in native human adipose-derived stem cells. Cell Biochem Biophys 67: 255–262.
29. Rochais F, Mesbah K, Kelly RG (2009) Signaling pathways controlling second heart field development. Circ Res 104: 933–942.
30. Watanabe Y, Kokubo H, Miyagawa-Tomita S, Endo M, Igarashi K, et al. (2006) Activation of Notch1 signaling in cardiogenic mesoderm induces abnormal heart morphogenesis in mouse. Development 133: 1625–1634.
31. Hickey EJ, Caldarone CA, McCrindle BW (2012) Left ventricular hypoplasia: a spectrum of disease involving the left ventricular outflow tract, aortic valve, and aorta. J Am Coll Cardiol 59: S43–54.
32. McBride KL, Riley MF, Zender GA, Fitzgerald-Butt SM, Towbin JA, et al. (2008) NOTCH1 mutations in individuals with left ventricular outflow tract malformations reduce ligand-induced signaling. Hum Mol Genet 17: 2886–2893.
33. Garg V, Muth AN, Ransom JF, Schluterman MK, Barnes R, et al. (2005) Mutations in NOTCH1 cause aortic valve disease. Nature 437: 270–274.
34. Luxan G, Casanova JC, Martinez-Poveda B, Prados B, D'Amato G, et al. (2013) Mutations in the NOTCH pathway regulator MIB1 cause left ventricular noncompaction cardiomyopathy. Nat Med 19: 193–201.
35. Boni A, Urbanek K, Nascimbene A, Hosoda T, Zheng H, et al. (2008) Notch1 regulates the fate of cardiac progenitor cells. Proc Natl Acad Sci U S A 105: 15529–15534.
36. de la Pompa JL, Epstein JA (2012) Coordinating tissue interactions: Notch signaling in cardiac development and disease. Dev Cell 22: 244–254.
37. Riley P, Anson-Cartwright L, Cross JC (1998) The Hand1 bHLH transcription factor is essential for placentation and cardiac morphogenesis. Nat Genet 18: 271–275.
38. Srivastava D, Thomas T, Lin Q, Kirby ML, Brown D, et al. (1997) Regulation of cardiac mesodermal and neural crest development by the bHLH transcription factor, dHAND. Nat Genet 16: 154–160.
39. Tsuchihashi T, Maeda J, Shin CH, Ivey KN, Black BL, et al. (2011) Hand2 function in second heart field progenitors is essential for cardiogenesis. Dev Biol 351: 62–69.
40. Jiang Y, Habibollah S, Tilgner K, Collin J, Barta T, et al. (2014) An induced pluripotent stem cell model of hypoplastic left heart syndrome (HLHS) reveals multiple expression and functional differences in HLHS-derived cardiac myocytes. Stem Cells Transl Med 3: 416–423.
41. Small EM, Krieg PA (2003) Transgenic analysis of the atrialnatriuretic factor (ANF) promoter: Nkx2-5 and GATA-4 binding sites are required for atrial specific expression of ANF. Dev Biol 261: 116–131.
42. Sepulveda JL, Belaguli N, Nigam V, Chen CY, Nemer M, et al. (1998) GATA-4 and Nkx-2.5 coactivate Nkx-2 DNA binding targets: role for regulating early cardiac gene expression. Mol Cell Biol 18: 3405–3415.
43. Sorensen AL, Jacobsen BM, Reiner AH, Andersen IS, Collas P (2010) Promoter DNA methylation patterns of differentiated cells are largely programmed at the progenitor stage. Mol Biol Cell 21: 2066–2077.

Acta Med. Okayama, 2014
Vol. 68, No. 3, pp. 157-162

Acta Medica Okayama
http://escholarship.lib.okayama-u.ac.jp/amo/

Original Article

Usefulness of High Mobility Group Box 1 Protein as a Plasma Biomarker in Patient with Peripheral Artery Disease

Susumu Oozawa[a]*, Shunji Sano[a], and Masahiro Nishibori[b]

Departments of [a]Cardiovascular Surgery, and [b]Pharmacology, Okayama University Graduate School of Medicine, Dentistry and Pharmaceutical Sciences, Okayama 700-8558, Japan

Atherosclerosis is often associated with chronic vascular inflammation. High-mobility group box 1 protein (HMGB1) plays various roles, not only as a transcriptional regulatory factor in the nucleus, but also as an inflammatory mediator. A previous study suggested that fibrinogen is an important factor associated with atherosclerosis progression. The present study was performed to examine the levels of plasma HMGB1 protein in atherosclerosis patients. We studied 24 patients with peripheral artery disease (PAD) with atherosclerosis, and 10 healthy controls. We found that the concentrations of HMGB1 were increased in the plasma of the patients with atherosclerosis, and there were significant correlations between the plasma HMGB1 and fibrinogen levels. Plasma HMGB1 may play a key role in the pathogenesis of clinical and experimental atherosclerosis.

Key words: HMGB1, fibrinogen, atherosclerosis, peripheral artery disease

Atherosclerosis is the one of the most common causes of cardiovascular disease. Although atherosclerosis is associated with hypertension, diabetes and hyperlipidemia, recent studies suggest an additional association with inflammation and the coagulation system.

High-mobility group box 1 protein (HMGB1) is a nuclear protein present in many cells. When inflammation occurs, HMGB1 is released into the extracellular space in both an active and a passive manner. It functions as a signal for inducing inflammation and as an activator for inducing the immune response [1, 2]. The action of extracellular HMGB1 appears to be dependent on its interactions with several cell surface receptors, *e.g.*, the receptor for advanced glycation end products (RAGE) and toll-like receptor 2/4 (TLR-2/4). Extracellular HMGB1 has been reported in a variety of clinical conditions associated with inflammation and reperfusion injury [3-6].

It's was suggested that atherosclerosis is characterized by a chronic inflammatory response to arterial wall injury [7]. RAGE is expressed in human atherosclerotic lesions [8]. Smooth muscle cells with atherosclerosis show increased expressions of HMGB1 and RAGE [9, 10]. RAGE expression is significantly up-regulated in macrophages associated with atherosclerotic lesions [8], and inhibition of RAGE signaling prevents the progression of atherosclerotic injury [11].

In the coagulation system, serum fibrinogen is one of the factors associated with blood coagulation and viscosity. Fibrinogen may therefore be closely related to atherosclerosis [8-10]. It was suggested that the mortality rate of individuals with cardiovascular disease is associated with high levels of serum fibrinogen [12]. Fibrinogen is essential for fibrin formation

Received September 20, 2013; accepted February 12, 2014.
*Corresponding author. Phone:+81-86-235-7357; Fax:+81-86-235-7431
E-mail:ohzawa-s@cc.okayama-u.ac.jp (S. Oozawa)

under the influence of thrombin and platelet aggregation [13]. In addition, fibrinogen synthesis is stimulated by cytokines from activated macrophages, and thus fibrinoge behaves as an acute-phase protein [14].

These observations suggest that fibrinogen, like HMGB1, might be associated with the coagulation and inflammation systems. In the present stud, we examined the expression of plasma HMGB1 in patients with atherosclerosis and we evaluated the correlation between plasma HMGB1 and the inflammatory or coagulation systems.

Materials and methods

The plasma levels of HMGB1 were measured in 10 healthy controls (age 66.3 ± 11.7 years, 7 males and 3 females) and 24 PAD patients (age 64.5 ± 17.4 years, 21 males and 3 females). All patients and volunteers provided informed consent, and the study was approved by the institutional review board at Okayama University Hospital (Okayama, Japan). First blood samples (0.5 mL) were collected from the subjects' peripheral vein and then centrifuged (3,000 rpm, 10 min) to obtain plasma samples. Second blood samples (0.5 mL) were collected using citric acid and centrifuged to obtain plasma samples. After centrifugation, these samples were stored at −80℃ until they were analyzed. The last blood samples (0.5 mL) were collected using EDTA 2Na for the blood cell counts.

The concentration of HMGB1 in plasma samples was determined using an enzyme-linked immunosorbent assay (ELISA) kit according to the manufacturer's protocol (Shino-Test, Sagamihara, Japan). The HMGB1 levels are expressed as nanograms per milliliter (ng/mL). We then analyzed the white blood cells count (WBC: $\times 10^4/mm^2$), C-reactive protein (CRP: mg/dL), platelet count (Plt: $\times 10^4/mm^2$), activated partial thromboplastin time (APTT: sec), and fibrinogen (Fib: mg/dL) using the standard methods established by the Department of the Central Clinical Laboratory, Okayama University Hospital.

The patients were divided into 2 groups according to the ankle brachial pressure index (ABI): the mild PAD group (ABI ≥ 0.6) and the severe PAD group (ABI < 0.6). All data are expressed as the mean ± SD. Group comparisons were performed using an analysis of variance (ANOVA) followed by the Mann-Whitney U-test. Correlation coefficients were determined using the Spearman rank test. In order to identify possible confounders of the correlation between HMGB1 and PAD both a univariate and a multivariate analysis with a multiple linear regression model were performed. A probability of < 0.05 was considered to be significant.

Results

HMGB1 expression in systemic circulation. The patients with PAD showed higher plasma levels of HMGB1 compared to the healthy controls (n = 10, median 4.63 ng/mL; 95% confidence interval [CI] 3.56–5.41). In addition, there were significant differences in the plasma HMGB1 levels between the mild (n = 12, median 6.16 (3.51–11.25; 95% CI) ng/mL; $p < 0.05$ vs. severe PAD group) and severe PAD patients (n = 12, median 16.18 ng/mL; 95% CI 3.18–29.00; $p < 0.01$ vs. control group) (Fig. 1).

Relationship between plasma HMGB1 and inflammatory or coagulation factors. The demographic data for the 24 subjects are presented in Table 1. The PAD grade also showed a significant correlation with the plasma level of fibrinogen (438 ± 99 mg/dL in the mild PAD group vs. 559 ± 151 mg/dL in the severe PAD group; $p < 0.05$). Table 2 shows the results of the multivariable analysis for factors correlated with plasma HMGB1 levels. Both the ABI ($p = 0.003$) and the plasma level of fibrinogen ($p < 0.001$) were significantly associated with the subjects' HMGB1 levels. However, CRP and other coagula-

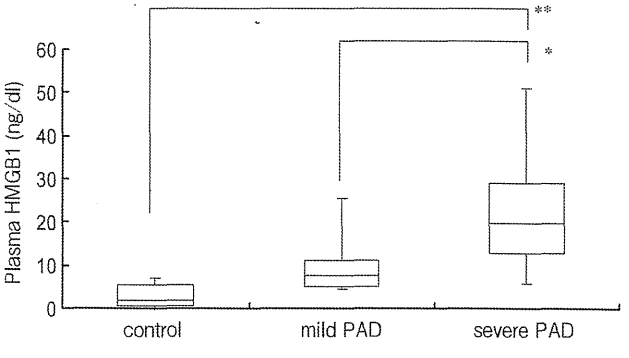

Fig. 1 The plasma levels of HMGB1 in atherosclerosis patients and relations between atherosclerosis progress and plasma levels of HMGB1. Data represent the median ± 95% confidence interval (CI). $^*p < .05$, $^{**}p < .01$ in comparison to the severe PAD group. PAD; peripheral artery disease.

Table 1 Comparison of baseline characteristics according- Fontaine in PAD Patients

PAD Patients Variables	mild PAD (n=12)	severe PAD (n=12)	p value
Male	9 (75.0)	12 (100.0)	
Age, years	63.9 ± 15.9	65.1 ± 18.0	0.869
Body weight, kg	63.3 ± 13.1	59.6 ± 12.2	0.504
Systoric BP, mmHg	145.4 ± 16.2	134.2 ± 12.4	0.109
Diastolic BP, mmHg	77.1 ± 8.0	77.6 ± 6.7	0.880
Ambulatory distance, m	174.3 ± 294.4	34.5 ± 30.2	0.116
ABI	0.72 ± 0.10	0.32 ± 0.15	<.001
Smoking	12 (100.0)	11	91.6
Medication for			
Hypertention	11 (91.6)	7 (83.3)	
Diabetes	7 (58.3)	3 (25.0)	
Hyperlipidemia	7 (58.3)	8 (32.0)	
Laboratory values			
WBC, $\times 10^4/mm^2$	6,536 ± 3,576	8,583 ± 3,623	0.209
Hb, mg/dl	12.1 ± 2.4	12.8 ± 2.4	0.509
Hct, %	36.6 ± 6.8	38.3 ± 6.6	0.556
Plt, $\times 10^4/mm^2$	22.2 ± 7.2	34.4 ± 19.7	0.078
APTT, sec	32.9 ± 4.8	31.8 ± 6.7	0.657
Fibrinogen, mg/dl	438 ± 99	559 ± 151	0.045
CRP, mg/dl	1.25 ± 2.13	1.38 ± 3.00	0.912
HMGB1, ng/ml	7.38 ± 6.09	19.08 ± 15.59	0.024

Data are expressed as mean ± SD or number (percentage).
PAD, peripheral artery disease; BP, blood pressure; ABI, ankle brachial pressure index; WBC, white blood cell number; Hb, hemoglobin; Hct; Plt, platelet number; PT, prothorombin time; APTT, active partial thromboplastin time; CRP, C-reactive protein.

Table 2 Correlation coefficients for HMGB1 in PAD patients

Variables	Correlation coefficients	p value
Age, years	−0.022	0.922
Body weight, kg	0.170	0.225
Systoric BP, mmHg	−0.288	0.231
Diastolic BP, mmHg	−0.301	0.210
Ambulatory distance, m	−0.194	0.353
ABI	−0.566	0.003
Smoking	0.124	0.555
Medication for		
Hypertention	−0.126	0.438
Diabetes	−0.231	0.307
Hyperlipidemia	−0.313	0.127
Laboratory values		
WBC, $\times 10^4/mm^2$	0.097	0.677
Hb, mg/dl	0.127	0.584
Hct, %	0.093	0.688
Plt, $\times 10^4/mm^2$	0.359	0.110
APTT, sec	0.211	0.371
Fibrinogen, mg/dl	0.754	<0.001
CRP, mg/dl	0.229	0.331

PAD, peripheral artery disease; WBC, white blood cell number; APTT, active partial thromboplast; CRP, C-reactive protein.

tion-related factors demonstrated no significant relationship with HMGB1.

Fig. 2 shows the relationships between the plasma HMGB1 and fibrinogen levels. The correlation coefficient was 0.455. Table 3 shows the results of the multivariable analysis for factors correlated with plasma HMGB1 levels. The only factor significantly associated with the HMGB1 level was fibrinogen ($p = .003$). The multiple stepwise regression analysis showed that fibrinogen was the only factor independently related to the HMGB1 levels ($R^2 = 0.353$) (Table 4).

Discussion

Atherosclerosis and extracellular HMGB1. Our results showed an association between atherosclerosis and increased plasma HMGB1 levels. Plasma HMGB1 levels have been reported to increase during inflammation, such as sepsis [1] and lung inflammation [3]. In the present study, the plasma HMGB1 levels in patients with PAD were much

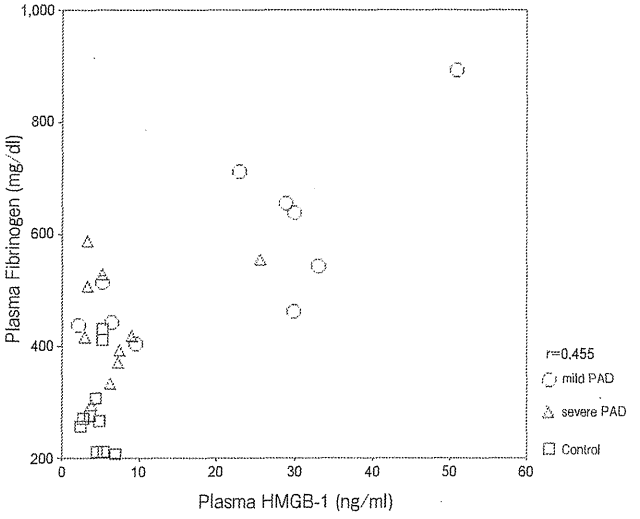

Fig. 2 The scatterplot shows that the relations between Plasma HMGB1 levels and fibrinogen for healthy control and peripheral artery disease. r, correlation coefficient.

Table 3 Multivariable analysis for correlates of HMGB1 levels

Characteristics	β	SE	p
ABI	−0.563	10.118	0.310
WBC	0.201	0.774	0.455
Hb	−0.133	4.412	0.892
Plt	−0.474	0.019	0.100
APTT	1.843	2.758	0.056
Fibrinogen	0.783	0.021	0.003
CRP	−1.400	3.006	0.065

Table 4 Multiple stepwise regression analysis for correlate of plasma HMGB1

Characteristics	β	SE	p
Fibrinogen	0.594	0.019	0.006

$R^2 = 0.353$

higher than those in healthy controls (Table 1). The source of circulating HMGB1 in atherosclerosis patients has not been determined, but 2 mechanisms are speculated to increase the general circulating HMGB1 levels. A local inflammatory secretory release of HMGB1 might be induced from immune responder cells such as monocytes, macrophages and endothelial cells with cytokine stimulation. Atherosclerotic lesions express high levels of HMGB1, thus leading to inflammation in atherosclerotic lesions [1, 2, 9]. However, the source of plasma HMGB1 may be not only immune responder cells but also vascular smooth muscle cells in atherosclerotic plaques [10].

In atherosclerotic plaques, endothelial cells and smooth muscle cells contain cytoplasmic HMGB1. HMGB1 is accumulated from the cytoplasm into secretory vesicles. However, atherosclerotic plaques contain extracellular HMGB1, which is released from necrotic cells [9]. While atherosclerotic inflammation continues, HMGB1 may be released into circulating blood.

It was suggested that HMGB1 is associated with the inflammatory and coagulation systems [15]. During the last stage of atherosclerosis, plaque rupture induces the formation of a thrombus. Endothelial cells lose their anti-coagulation properties and adhere to platelets. As shown in Fig. 1, the plasma levels of HMGB1 correlate with the progression of atherosclerosis. Normally, patients with severe PAD have severe local infection and gangrene of the foot. However, our present findings indicate that the infection-related factors WBC and CRP were not significantly related to the ABI degree, and thus the plasma level of HMGB1 may be independent from local infection or necrosis. Therefore, the extracellular HMGB1 secreted from atherosclerotic lesions and local HMGB1 may contribute platelets to the formation of thrombosis and the progression of atherosclerosis.

Atherosclerosis and fibrinogen. Atherosclerosis has been demonstrated to be associated with inflammatory processes in the vascular walls [15, 16]. The activity and progression of atherosclerosis is influenced by vascular inflammation [17]. Fibrinogen is an acute protein marker as well as a coagulation factor and has various other functions such as determining the blood viscosity and stimulating vascular smooth muscle cell migration and proliferation. Fibrinogen provides an indirect measure of cytokine-dependent inflammatory processes in the atherosclerotic wall. In addition to its role as a nonspecific marker of inflammation, fibrinogen is involved in atherogenesis and thrombogenesis by acting as a bridging molecule for many types of cell-to cell adhesion events that are critical for atherogenesis [18].

Fibrinogen plays a central role in the coagulation cascade and has a critical impact on the formation of fibrin clots following the rupture of an atherosclerotic

plaque [19]. The agents used to treat atherosclerosis, such as statins and angiotensin-converting enzyme inhibitors, which improve clinical outcomes in primary and secondary prevention [20], decrease the fibrinogen levels [21]. It was thus suggested that increased plasma fibrinogen is one of the risk factors for PAD [8-10]. In the present study, there was a significant correlation between HMGB1 and fibrinogen (Fig. 2).

In addition, the present subjects' fibrinogen levels were independently correlated with HMGB1 levels (Table 3). The multiple stepwise regression analysis showed that fibrinogen's R^2 (multiple regression coefficient) was 0.353, and the p-value for fibrinogen was 0.006 (Table 4). Our results may indicate a causal relationship between HMGB1 and fibrinogen, and thus, high levels of plasma HMGB1 and fibrinogen may induce atherosclerotic progression. A prior study suggested that HMGB1 is a potential biomarker for subclinical inflammation [1]. HMGB1 may be a good candidate as a marker for atherosclerosis.

Here we found that the concentration of HMGB1 was increased in the patients with atherosclerosis, and the level of plasma HMGB1 was correlated with that of fibrinogen. We therefore speculate that the plasma HMGB1 level is increased in atherosclerotic patients, and a significant correlation between the plasma HMGB1 and plasma fibrinogen levels will be examined and perhaps confirmed in future studies.

However, our study also has some technical limitations. First, we evaluated a very small number of patients. Comparisons of large numbers of PAD patients may better elucidate the relationships among plasma HMGB1, fibrinogen and PAD. Second, we used only the ABI for our atherosclerosis classification. The ABI values were obtained with an oscillometric automated device, and small differences in the device's measurements may have altered the final numerical ABI values. Using another measurement device such as a skin perfusion pressure (SPP) or transcutaneous partial pressure ($tcPO_2$) device may better clarify these relations. Third, we do not yet know the mechanisms underlying how HMGB1 is related to atherosclerosis. A longitudinal study is needed to clarify the causal relationships among HMGB1, fibrinogen levels, and atherosclerosis progression. We also do not know whether HMGB1 as a biomarker has a strong relationship with atherosclerosis progression. Further investigations of the role of HMGB1 may make it possible to identify a novel biomarker for atherosclerosis.

Acknowledgments. We thank Dr. Nobuya Ohara and Mrs. Rika Takamoto for their technical assistance.

References

1. Wang H, Yang H and Tracey KJ: Extracellular role of HMGB1 in inflammation and sepsis. J Intern Med (2004) 255: 320-331.
2. Wang H, Bloom O, Zhang M, Vishnubhakat JM, Ombrellino M, Che J, Frazier A, Yang H, Ivanova S, Borovikova L, Manogue KR, Faist E, Abraham E, Andersson J, Andersson U, Molina PE, Abumrad NN, Sama A and Tracey KJ: HMG-1 as a late mediator of endotoxin lethality in mice. Science (1999) 285: 248-251.
3. Ueno H, Matsuda T, Hashimoto S, Amaya F, Kitamura Y, Tanaka M, Kobayashi A, Maruyama I, Yamada S, Hasegawa N, Soejima J, Koh H and Ishizaka A: Contributions of high mobility group box protein in experimental and clinical acute lung injury. Am J Respir Crit Care Med (2004) 170: 1310-1316.
4. Tsung A, Sahai R, Tanaka H, Nakao A, Fink MP, Lotze MT, Yang H, Li J, Tracey KJ, Geller DA and Billiar TR: The nuclear factor HMGB1 mediates hepatic injury after murine liver ischemia-reperfusion. J Exp Med (2005) 201: 1135-1143.
5. Liu K, Mori S, Takahashi HK, Tomono Y, Wake H, Kanke T, Sato Y, Hiraga N, Adachi N, Yoshino T and Nishibori M: Anti-high mobility group box 1 monoclonal antibody ameliorates brain infarction induced by transient ischemia in rats. FASEB J (2007) 21: 3904-3916.
6. Oozawa S, Mori S, Kanke T, Takahashi H, Liu K, Tomono Y, Asanuma M, Miyazaki I, Nishibori M and Sano S: The Effects of HMGB1 on Ischemia-Reperfusion Injury in the Rat Heart. Circ J (2008) 72: 1178-1184.
7. Li W, Sama AE and Wang H: Role of HMGB1 in cardiovascular diseases. Curr Opin Pharmacol (2006) 6: 130-135.
8. Basta G: Receptor for advanced glycation endproducts and atherosclerosis: From basic mechanisms to clinical implications. Atherosclerosis (2008) 196: 9-21.
9. Kalinina N, Agrotis A, Antropova Y, DiVitto G, Kanellakis P, Kostolias G, Ilyinskaya O, Tararak E and Bobik A: Increased expression of the DNA-binding cytokine HMGB1 in human atherosclerotic lesions: role of activated macrophages and cytokines. Arterioscler Thromb Vasc Biol (2004) 24: 2320-2325.
10. Porto A, Palumbo R, Pieroni M, Aprigliano G, Chiesa R, Sanvito F, Maseri A and Bianchi ME: Smooth muscle cells in human atherosclerotic plaques secrete and proliferate in response to high mobility group box 1 protein. FASEB J (2006) 20: 2565-2566.
11. Cuccurullo C, Iezzi A, Fazia ML, De Cesare D, Di Francesco A, Muraro R, Bei R, Ucchino S, Spigonardo F, Chiarelli F, Schmidt AM, Cuccurullo F, Mezzetti A and Cipollone F: Suppression of RAGE as a basis of simvastatin-dependent plaque stabilization in type 2 diabetes. Arterioscler Thromb Vasc Biol. (2006) 26: 2716-2723.
12. Mannucci PM: Recent progress in the pathophysiology of fibrinogen. Eur Heart J (1995) 16: 25-30.
13. Ernst E: Fibrinogen: Its Emerging Role as a Cardiovascular Risk Factor. Angiology (1994) 45: 87-93.
14. Fiuza C, Bustin M, Talwar S, Tropea M, Gerstenberger E, Shelhamer JH and Suffredini AF: Inflammation-promoting activity of HMGB1 on human microvascular endothelial cells. Blood (2003)

101: 2652-2660.
15. Ross R: Atherosclerosis: an inflammatory disease. N Engl J Med (1999) 340: 115-126.
16. Libby P, Ridker P and Maseri A: Inflammatory and atherosclerosis. Circulation (2002) 105: 1135-1143.
17. Blake GJ and Ridker PM: Novel clinical markers of vascular wall inflammation. Circ Res (2001) 89: 763-771.
18. Naito M, Hyashi T, Kuzuya M, Funaki C, Asai K and Kuzuya F: Effects of fibrinogen and fibrin on the migration of vascular smooth muscle cells in vitro. Atherosclerosis (1990) 83: 9-14.
19. Koenig W: Fibrinogen in cardiovascular disease: an update. Thromb Haemost (2003) 89: 601-609.
20. Afilalo J, Duque G, Steele R, Jukema JW, Craen AJ and Eisenberg M: Statins for secondary prevention in elderly patients: a hierarchical Bayesian meta-analysis. J Am Coll Cardiol (2008) 51: 37-45.
21. Roy SN, Mukhopadhyay G and Redman CM: Regulation of fibrinogen assembly Transfection of Hep G2 cells with B beta cDNA specifically enhances synthesis of the three component chains of fibrinogen. J Biol Chem (1990) 265: 6389-6393.

ASIAN CARDIOVASCULAR & THORACIC ANNALS

Asian Cardiovascular & Thoracic Annals
0(0) 1

DOI: 10.1177/0218492314542288
aan.sagepub.com
SAGE

Anomalous right subclavian artery from pulmonary artery

Ko Yoshizumi, Shingo Kasahara and Shunji Sano

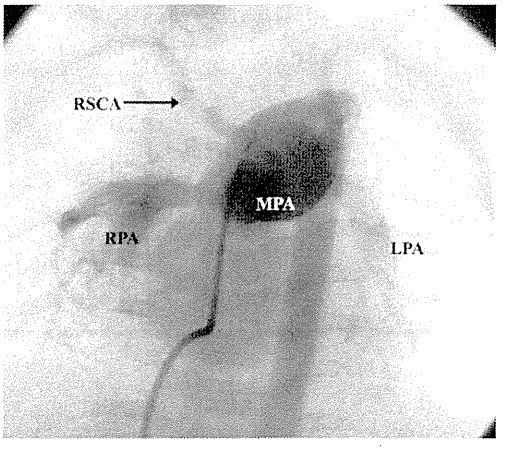

Figure 1. Main pulmonary angiogram demonstrating the descending aortic artery through a patent arterial duct from the main pulmonary artery (MPA), and the right subclavian artery (RSCA) originating from the main pulmonary artery. LPA: left pulmonary artery; RPA: right pulmonary artery.

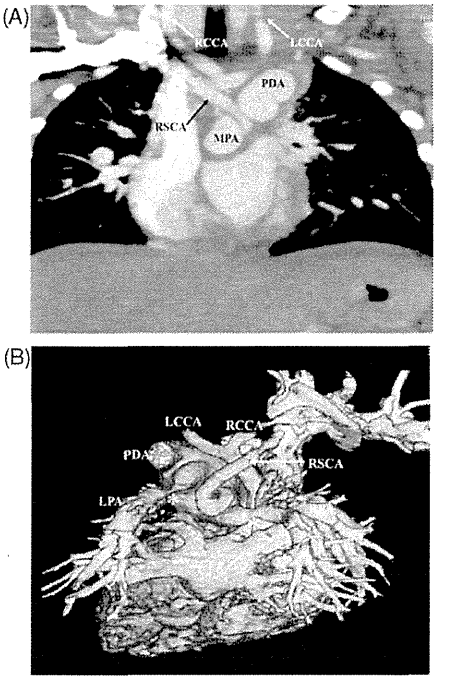

Figure 2. (A) Multidetector computed tomography angiogram showing the aberrant right subclavian artery (RSCA) from the main pulmonary artery (MPA). (B) Three-dimensional reconstructed image of the multidetector computed tomography clearly displayed the right subclavian artery (RSCA) arising from the main pulmonary artery, interrupted aortic arch, and the banding on both pulmonary arteries (asterisk). LCCA: left common carotid artery; LPA: left pulmonary artery; PDA: patent ductus arteriosus; RCCA: right common carotid artery; RPA: right pulmonary artery.

A 3-day-old girl born at 39 weeks gestation weighing 2804 g was referred for cardiac evaluation on the 3rd day of life due to a heart murmur and tachypnea. She was found to have an interrupted aortic arch type B, a ventricular septal defect, a dysplastic aortic valve, 2 adequate-sized ventricles, and a patent arterial duct on echocardiography. She was immediately started on a prostaglandin E_1 infusion. We planned a staged biventricular repair with the combined Norwood and Rastelli procedures. The patient underwent bilateral pulmonary artery banding for regulation of high pulmonary flow on day 10 after birth, as an initial palliative treatment. An angiogram (Figure 1) and multidetector computed tomography (Figure 2A, 2B) after the initial palliative operation revealed a rare anomaly: an aberrant right subclavian artery that originated from the junction of the main pulmonary artery and the right pulmonary artery.

Conflict of interest statement

None declared.

Funding

This research received no specific grant from any funding agency in the public, commerical, or not-for-profit sectors.

Division of Cardiovascular Surgery, Okayama University Graduate School of Medicine, Dentistry and Pharmaceutical Sciences, Okayama, Japan

Corresponding author:
Ko Yoshizumi, Okayama University Graduate School of Medicine, Dentistry and Pharmaceutical Sciences Division of Cardiovascular Surgery, Kita-ku Shikata-cho 2-5-1, Okayama, Japan.
Email: yoshizumi0709@gmail.com

European Journal of Cardio-Thoracic Surgery 45 (2014) 549–555
doi:10.1093/ejcts/ezt465 Advance Access publication 1 November 2013

ORIGINAL ARTICLE

Repair of Ebstein's anomaly in neonates and small infants: impact of right ventricular exclusion and its indications†

Shunji Sano*, Yasuhiro Fujii, Shingo Kasahara, Yosuke Kuroko, Atsushi Tateishi, Ko Yoshizumi and Sadahiko Arai

Department of Cardiovascular Surgery, Okayama University Hospital, Okayama, Japan

* Corresponding author. Department of Cardiovascular Surgery, Okayama University Hospital, 2-5-1 Shikata-cho, Kita-ku, Okayama City, Okayama 700-8558, Japan. Tel: +81-86-2357359; fax: +81-86-2357431; e-mail: s_sano@cc.okayama-u.ac.jp (S. Sano).

Received 15 January 2013; received in revised form 29 June 2013; accepted 8 July 2013

Abstract

OBJECTIVES: In cases of severe Ebstein's anomaly, it is essential to determine whether biventricular repair (BVR) or single-ventricle palliation is feasible. Since 1999, in our institution, we have used the novel technique comprising tricuspid valve (TV) closure and right ventricular and right atrial (RV/RA) exclusion to reduce the deleterious effects of an enlarged RV in patients with severe Ebstein's anomaly. However, in cases with good RV function, primary BVR is performed. In the present study, we describe our surgical strategy in the treatment of severely symptomatic neonates with Ebstein's anomaly.

METHODS: From June 1999 to October 2011, 12 neonates with a severely symptomatic Ebstein's anomaly underwent surgical repair. The mean age at the first operation was 29 ± 25 (range, 5–92) days; and the mean body weight was 2.8 ± 0.5 (range, 2.0–4.1) kg. The associated anomalies included pulmonary atresia with an intact ventricular septum in 7, critical pulmonary stenosis in 1, ventricular septal defect in 3 and coarctation of the aorta in 1 patient. The mean cardio-thoracic ratio (CTR) was 80 ± 14% (range, 57–98%). Preoperatively, 9 patients had grade IV tricuspid regurgitation (TR), as detected by echocardiography, and 6 required ventilator support.

RESULTS: Five patients underwent primary BVR. Seven patients underwent staged palliation using a modified Blalock-Taussig shunt (BT shunt) with/without RV/RA exclusion. There was 1 case each of hospital death and late death. The median follow-up duration in the present study was 6.5 years. Among the 8 patients who underwent TV repair, postoperative TR was trivial or mild in 6 patients, moderate in 1 and absent in 1. After surgery, the mean CTR and serum B-type natriuretic peptide levels decreased to 59 ± 14% (range, 45–70%) and 46 ± 28 (range, 12–83) pg/dl, respectively.

CONCLUSIONS: Critically ill neonates with Ebstein's anomaly can be successfully treated using RV/RA exclusion combined with a modified BT shunt in cases where RV function is poor. However, in cases of good RV function, we recommend the use of primary BVR.

Keywords: Ebstein's anomaly • Neonate • Cardiac surgery • Right ventricular exclusion

CONGENITAL

INTRODUCTION

Management of a neonate with symptomatic Ebstein's anomaly is a very challenging situation for paediatric cardiologists and paediatric cardio-thoracic surgeons, as these patients tend to have a higher risk of early mortality compared with neonates with hypoplastic left heart syndrome, even in institutions with the most experienced surgeons [1, 2]. Tricuspid valve (TV) repair for symptomatic neonatal Ebstein's anomaly is reportedly an extremely high-risk procedure with a high early mortality rate. TV repair outcomes in patients with Ebstein's anomaly and right ventricular (RV) outflow obstruction are particularly poor. In 1991, Starnes *et al.* [3] introduced an innovative surgical treatment for severe neonatal Ebstein's anomaly, referred to as the Starnes operation. This procedure involved the univentricularization of the heart by TV closure using a fenestrated patch and a modified Blalock-Taussig shunt (BT shunt). Acceptable survival rates have been reported for neonates or early infants with Ebstein's anomaly who underwent the Starnes operation. Since 1998, in our institution, we have used a novel technique comprising TV closure and free wall resection of the RV and right atrium (RV/RA exclusion) to create a single left ventricle (LV) in patients with isolated RV dysfunction to reduce the deleterious effects of an enlarged RV [4]. We have applied this technique since 1999 to patients with severe Ebstein's anomaly.

Appropriate patient selection and determination of which patients should be treated with a univentricular or biventricular approach have been problematic, since accurately estimating RV function is difficult despite the development of diagnostic procedures, including echocardiography and magnetic resonance imaging. Some doctors state that all neonates with symptomatic Ebstein's anomaly and pulmonary obstruction should undergo the Starnes operation, which has been accepted in most institutions worldwide. However, in our institution, an effort has always been

†Presented at the 26th Annual Meeting of the European Association for Cardio-Thoracic Surgery, Barcelona, Spain, 27–31 October 2012.